PNAS RESEARCH ARTICLE | ECOLOGY

Threatened North African seagrass meadows have supported green turtle populations for millennia

Willemien de Kock[a,b,1], Meaghan Mackie[c,d], Max Ramsøe[c], Morten E. Allentoft[e,f], Annette C. Broderick[g], Julia C. Haywood[g], Brendan J. Godley[g], Robin T. E. Snape[g,h], Phil J. Bradshaw[g], Hermann Genz[i], Matthew von Tersch[j], Michael W. Dee[k], Per J. Palsbøll[b,l], Michelle Alexander[j,2], Alberto J. Taurozzi[c,2], and Canan Çakırlar[a,2]

Edited by Pablo Marquet, Pontificia Universidad Catolica de Chile, Santiago, Chile; received December 9, 2022; accepted May 25, 2023

***"Protect and restore ecosystems and biodiversity"* is the second official aim of the current UN Ocean Decade (2021 to 2030) calling for the identification and protection of critical marine habitats. However, data to inform policy are often lacking altogether or confined to recent times, preventing the establishment of long-term baselines. The unique insights gained from combining bioarchaeology (palaeoproteomics, stable isotope analysis) with contemporary data (from satellite tracking) identified habitats which sea turtles have been using in the Eastern Mediterranean over five millennia. Specifically, our analysis of archaeological green turtle (*Chelonia mydas*) bones revealed that they likely foraged on the same North African seagrass meadows as their modern-day counterparts. Here, millennia-long foraging habitat fidelity has been directly demonstrated, highlighting the significance (and long-term dividends) of protecting these critical coastal habitats that are especially vulnerable to global warming. We highlight the potential for historical ecology to inform policy in safeguarding critical marine habitats.**

sea turtles | bioarchaeology | stable isotope analysis | paleoproteomics | historical ecology

Significance

The persistence of most species and their key habitats is intimately tied together. Sea turtles famously exhibit a strong fidelity to their natal rookery where they return to nest. While satellite tracking has provided evidence of foraging-ground fidelity, this approach is limited to a small number of turtles observed over a few years. Incorporating the bioarchaeological record, we found that Mediterranean green turtles have been utilizing the same North African seagrass meadows for at least ~3,000 y. This enables site fidelity to be established at the generational level, uncovering habitat significance over timescales beyond the Anthropocene. Our results validate this concept and open the possibility of its application to other species, facilitating species management, thus informing biodiversity conservation.

Many endangered species return with high fidelity to habitats that are crucial for the species' persistence; habitats that often are threatened as well. In many cases, modern ecology is subject to the *Shifting Baselines* paradigm (1, 2), i.e., the generational shift of the reference point of a healthy ecosystem, resulting in an unknown baseline. Approaches that extend the timescales of ecological assessments can remove such "ecological conjecture" in conservation planning (3), and thus aid in predicting species adaptability in terms of habitat use (4). Palaeoecology aims at inferring ecological interactions at historical and palaeological timescales (5), but has yet not been applied to identify critical foraging habitats and their use over the long term, thus circumventing the issue of shifting baselines and informing management of endangered species and their habitats.

Sea turtles undertake iconic migrations between their natal nesting beaches to often distant, critical foraging areas. Two species of sea turtle nest and breed in the Mediterranean, the green turtle (*Chelonia mydas*) and the loggerhead turtle (*Caretta caretta*). The former nests solely in the Levant, where the vast majority of nests are located in Turkey and Cyprus (6, 7). In contrast, *C. caretta* nesting is widespread in the Mediterranean (8). *C. mydas* and *C. caretta* are listed on the IUCN red list as globally *endangered* (9) and *vulnerable* (10), respectively. Although both species show signs of recovery in the Mediterranean, *C. caretta* is listed regionally as *least concern* (8, 10), but the status of the species is "conservation dependent" (8). Foraging site fidelity has a positive relationship with breeding and feeding success in a number of migratory species (11–13). In sea turtles, selective pressure has presumably resulted in individuals imprinting on a specific feeding area instead of feeding in potentially riskier unknown habitats (14). Mediterranean sea turtles show high fidelity to specific foraging grounds, to which they return post breeding (15). It is unknown how long these populations have been utilizing these same areas, and such data could help us assess the importance of these habitats in the present and future.

Sea turtle remains are found in archaeological sites along the Levantine coast (eastern Mediterranean, Fig. 1) from the Neolithic (~11,700 to 7,800 years B.P.) to the Late Iron Age (~2,700 - 2,500 years B.P.) (16). We analyzed sea turtle bones from three Levantine archaeological settlements dating back to the Middle and Late Holocene (Fig. 1); *Kinet Höyük* (~2,700 years B.P.), *Tell Fadous-Kfarabida* (~4,700 years B.P.), and *Tell el-Burak* (~2,700 years B.P.). Evidence of cut marks on bones indicates that at these localities sea turtles were exploited for consumption. The sea turtle remains are assumed to originate from nearby nesting or breeding populations, given the proximity of these locales to present-day nesting sites. Despite zooarchaeological evidence of human–turtle interactions in the Levant over millennia, the dietary and feeding habitats

The authors declare no competing interest.

This article is a PNAS Direct Submission.

[1]To whom correspondence may be addressed. Email: w.de.kock@rug.nl.

[2]M.A., A.J.T., and C.Ç. contributed equally to this work.

This article contains supporting information online at https://www.pnas.org/lookup/suppl/doi:10.1073/pnas.2220747120/-/DCSupplemental.

Published July 17, 2023.

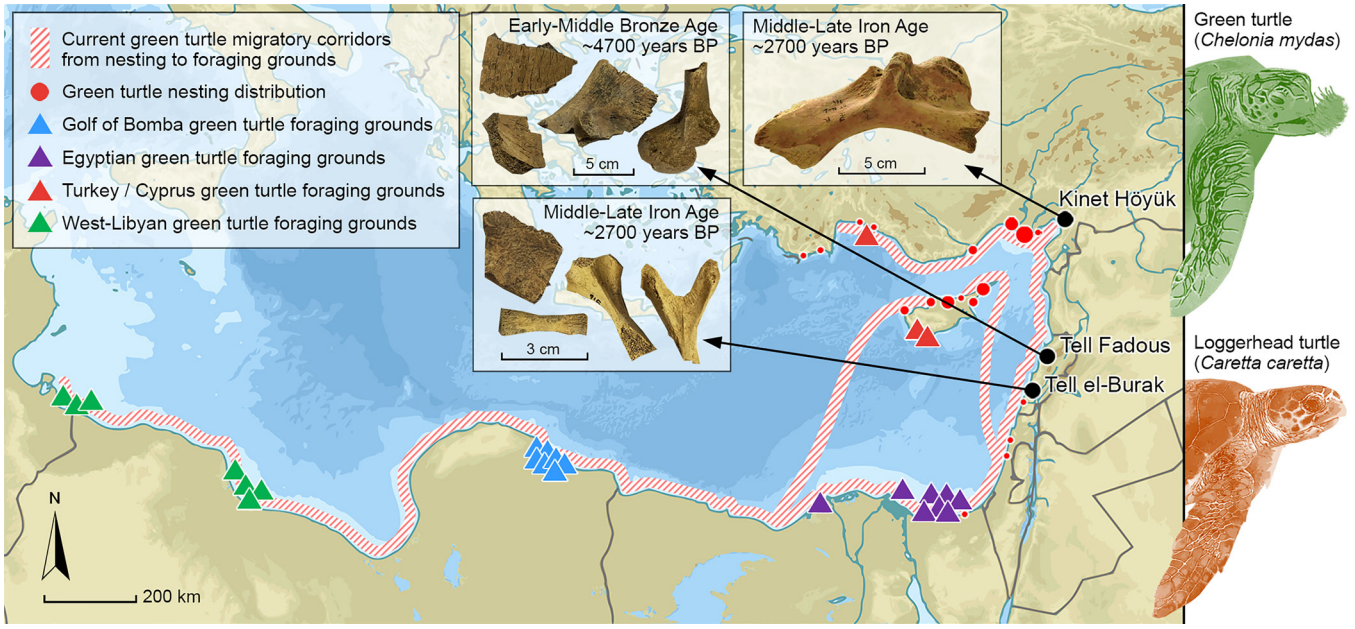

Fig. 1. Map of the Eastern Mediterranean. Three archaeological sites with sea turtle remains are marked, with an indication of the assemblage nature (highly fragmented at the southern Levantine sites) and bone elements analyzed at each site. Modern Mediterranean green turtle postnesting migration routes back to foraging grounds (white and red stripes) are taken from Stokes et al. (6) as well as the nesting distributions (red circles): the largest circles indicate 100 nests or more per year, and the smallest circles indicate less than 50 nests. Gulf of Bomba (n = 7, blue triangles), Egyptian (n = 8, purple triangles), Turkey/Cyprus (n = 3, pink triangles), and West Libyan (n = 7, green triangles) green turtle foraging grounds are presented as the final location of satellite-tracked modern turtles (17). Images of the two sea turtle species which nest and breed in the Mediterranean (*C. mydas* and *C. caretta*) are shown. Figure created with assistance from S.E. Boersma.

of these ancient sea turtles remain unknown, particularly as the species of the majority of turtle remains are unknown. We demonstrate how combining bioarchaeological data [Zooarchaeology by Mass-Spectrometry (ZooMS) species identification, LC–MS/MS shotgun proteomic sequencing, stable isotope analysis] from ancient samples with modern data (satellite tracking, stable isotope analysis) enabled direct identification of sea turtle breeding and foraging distributions in the eastern Mediterranean over several millennia, predating contemporary records.

Additional ZooMS Biomarkers Increase Species Identification Rate

Osteological and osteometrical species identification of *C. mydas* and *C. caretta* is possible from the humerus, femur, and coracoideum (18) but infeasible for fragmented material. However, species can be identified using collagen peptide biomarkers, which are applicable to highly fragmented material (19). The majority of the 124 archaeological turtle remains we analyzed were undiagnosable fragments (Fig. 1). Biomarkers that identify extant sea turtle species have been identified (20) using palaeoproteomics and ZooMS (21). We applied nanoscale liquid chromatography–tandem mass spectrometry (nanoLC–MS/MS) in four *C. caretta* reference specimens in order to resolve missing positions in the existing (20) Type I collagen (COL1) sequence by 84% (from 381 missing positions to 61, *SI Appendix*). We also found seven additional biomarkers that distinguished between *C. mydas* and *C. caretta* (Fig. 2), allowing us to confidently identify ~90% of the archaeological specimens. Including putative identifications at a lower level of confidence (Datasets S1 and S2), the species identification rate was ~98%, a significant improvement on previous methods (Fig. 3*A*). Restricting the assessment to *confident* species identifications only, the sea turtle material at the archaeological sites comprised 100% *C. mydas* (*Kinet Höyük*), 15% *C. mydas*, 70% *C. caretta* and 15% unidentified (*Tell Fadous-Kfarabida*), and 80% *C. caretta* and 20% unidentified (*Tell el-Burak*, Fig. 3*B*).

The ability to identify such a high proportion of the archaeological remains was instrumental to this study. The seven unique peptide biomarkers provide a cost-effective method to distinguish between *C. mydas* and *C. caretta* remains, species which often are sympatric. These peptides also serve as a useful starting point for finding additional proteomic differences among other extant sea turtle species. Given that the ZooMS results were consistent with the stable isotope data (SIA, see below) in regards to species identification, *less confident* ZooMS identifications were included in our analysis as well. The species composition in the archaeological samples at the three sites indicates that sea turtle breeding distribution along the Levant has remained similar throughout the past ~2,700 to 4,700 y, with *C. mydas* turtles present in the Northern Levant, decreasing in prevalence toward the South (6) (Fig. 3).

Stable Isotopes Reveal Ancient Mediterranean Sea Turtle Diet

Sea turtles migrate between breeding and foraging grounds, spending most of their time in the latter only, to breed every few years. Today most postbreeding *C. mydas* from Cyprus and Turkey migrate along specific corridors while en route to the foraging grounds at the North African coast [Fig. 1, (6, 17)]. Adult *C. caretta* undertake similar migrations between foraging and breeding grounds (22). More broadly, *C. caretta* from the Levant forage mostly in the Eastern Mediterranean and on the Tunisian plateau in the Strait of Sicily and, at rare occasions, in the Adriatic Sea. In contrast, *C. caretta* tracked from western Greece forage largely in the Adriatic Sea and on the Tunisian Plateau (22); however, their omnivorous diet makes differentiating highly specific foraging grounds more difficult. Sea turtle bone deposits annual growth layers that contain isotopic signatures reflecting the foraging from several years to the lifetime of the

A

Peptide Code	Standardised name	mass m/z		Peptide amino acid sequence		Post-Translational Modifications
		C. mydas	*C. caretta*	*C. mydas*	*C. caretta*	
from Harvey et al. 2019						
A1T55/T66	COL1α1 586-618	2843/59.3	2869/85.3	GLTGPIGPPGPAGAPGDKGEAGPSGPSG**S**TGAR	GLTGPIGPPGPAGAPGDKGEAGPSGPSG**P**TGAR	2x Hydroxyproline, 3x Hydroxyproline
A1T79	COL1α1 889-906	1516.7	1490.7	GETGPAGPAGPAGAG**P**R	GETGPAGPAGPAGA**A**R	-
A2T65/66	COL1α2 586-618	2353.1	2341.1	GDTGPVGRPGEQGIVGPPGF**T**GEK	GDTGPVGRPGEQGIVGPPGF**T**GEK	2x Hydroxyproline
Novel biomarkers						
A1T30/31	COL1α1 324-341	1731.84	1717.81	GFPGSDGISGPKGP**T**GER	GFPGSDGISGPKGP**S**GER	Hydroxyproline
A1T63/64/65	COL1α1 713-740	2598.86	2612.88	VGPPGPSGNIGLPGPPGPSGKEG**S**KGPR	VGPPGPSGNIGLPGPPGPSGKEG**T**KGPR	3x Hydroxyproline
A1T73	COL1α1 825-844	1768.95	1742.91	GPPGPVGPPGLAGP**P**GEAGR	GPPGPVGPPGLAGP**A**GEAGR	2x Hydroxyproline
A1T78/79	COL1α1 893-914	1960.07	1934.03	NGDRGETGPAGPAGPAGPAG**P**R	NGDRGETGPAGPAGPAGPAG**A**R	Deamidation
A2T35	COL1α2 393-402	920.08	881.99	VGPI**G**PAGPR	VGPT**G**AAGPR	-
A2T35/36	COL1α2 393-414	2104.37	2066.27	VGPI**G**PAGPRGEPGNIGFPGPK	VGPT**G**AAGPRGEPGNIGFPGPK	2x Hydroxyproline, Deamidation
A2T50/51	COL1α2 574-587	1327.46	1355.52	GLPGLRGE**A**GATGR	GLPGLRGE**V**GATGR	Hydroxyproline

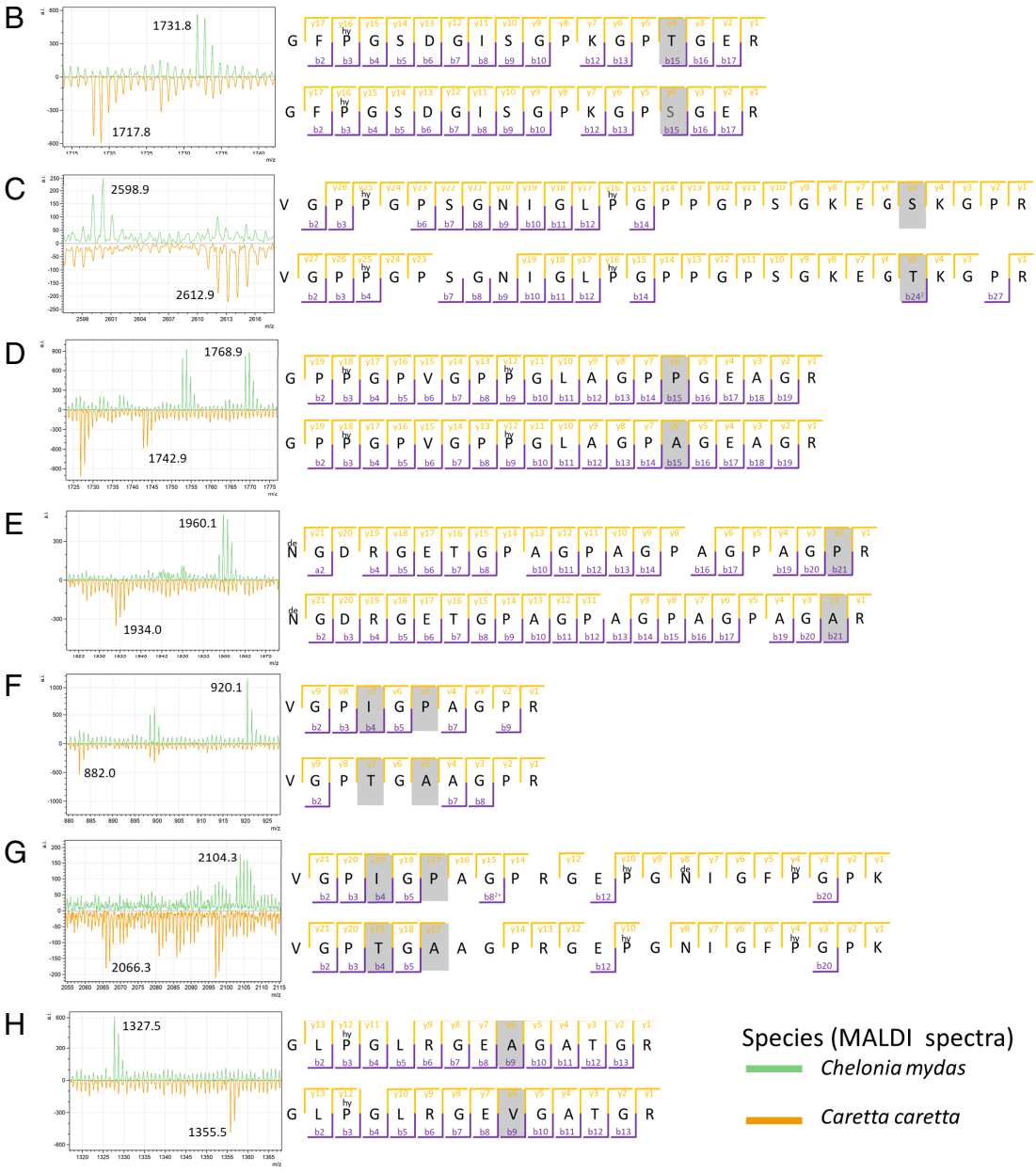

Fig. 2. (*A*) Published (20) and unique ZooMS biomarkers distinguishing *C. mydas* and *C. caretta*. The mass-to-charge ratio (m/z) displayed for each biomarker is the sum of the mass of the peptide amino acid sequence and any mass shifts due to potential posttranslational modifications, namely hydroxyproline (+16) and deamidation (+1). MALDI spectra for each unique ZooMS biomarker (*B*–*H*) denoting the ion coverage from nanoLC–MS/MS next to the spectra for each species (*C. mydas*, in green; *C. caretta* in orange).

individual (23, 24); when sampled, a time-average is achieved. We obtained $\delta^{13}C$ and $\delta^{15}N$ data from bone collagen in 74 archaeological samples, among which we obtained $\delta^{34}S$ values in 71 samples. Of these, 41 passed strict quality filtering for sulfur (25, 26). Stable isotope values differed ($P \leq 0.05$) between species and archaeological sites (Fig. 4 *A*–*C* and *SI Appendix*), with higher $\delta^{13}C$ values, and lower $\delta^{15}N$ and $\delta^{34}S$ values in *C. mydas compared to C. caretta.* The higher trophic level (higher $\delta^{15}N$ values) of archaeological *C. caretta* com-

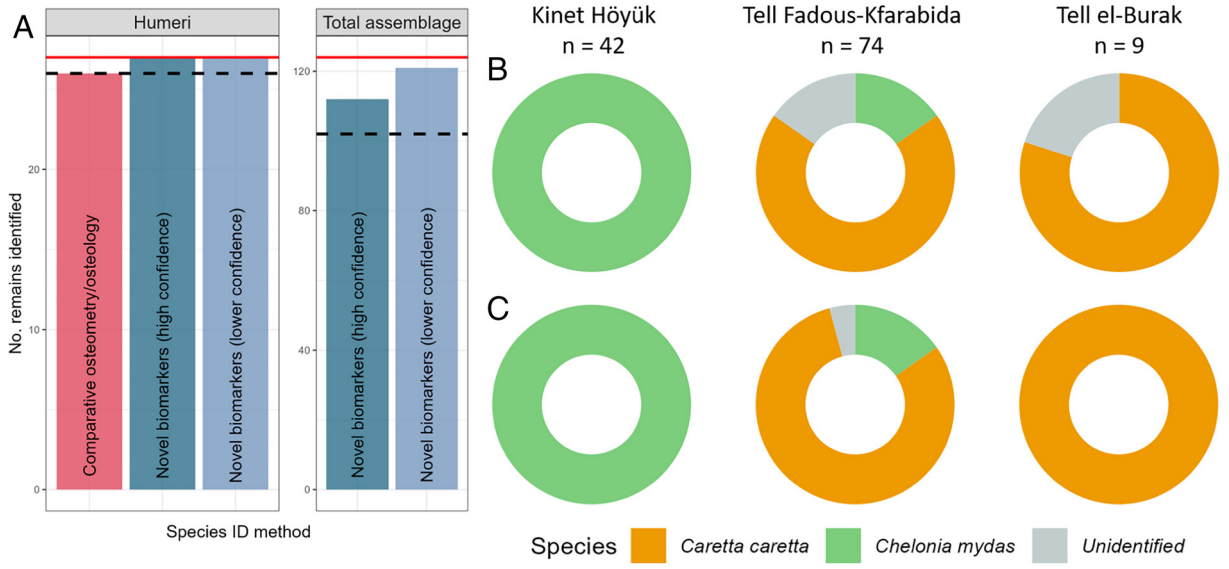

Fig. 3. (*A*) Comparisons between species identification methods for sea turtles from turtle humeri (n = 27) and our total bone assemblage (n = 124). The *dashed black line* indicates the number of remains identified by the published COL1α1 586 to 618 (20) peptide, the *red line* indicates the total experiment number for each facet. Comparative osteometry/osteology was not possible on the total assemblage due to lack of existing morphological identification criteria and the shattered nature of the remains. Donut charts of sea turtle species composition at three Levantine archaeological sites are shown in *B* for *confident* ZooMS identification with our 7 unique biomarkers, and in *C* for *less confident* ID (i.e., visible peaks that did not make the mMass peak picking threshold).

pared to *C. mydas* reflects the omnivorous diet of Mediterranean *C. caretta* (27). Samples from *Kinet Höyük* showed the same trend over samples from *Tell-Fadous-Kfarabida*, which was anticipated given the species distribution of the two sites. Ancient *C. mydas* populations also differed significantly between Iron Age *Kinet Höyük* and Bronze Age *Tell-Fadous-Kfarabida* in all measured stable isotope

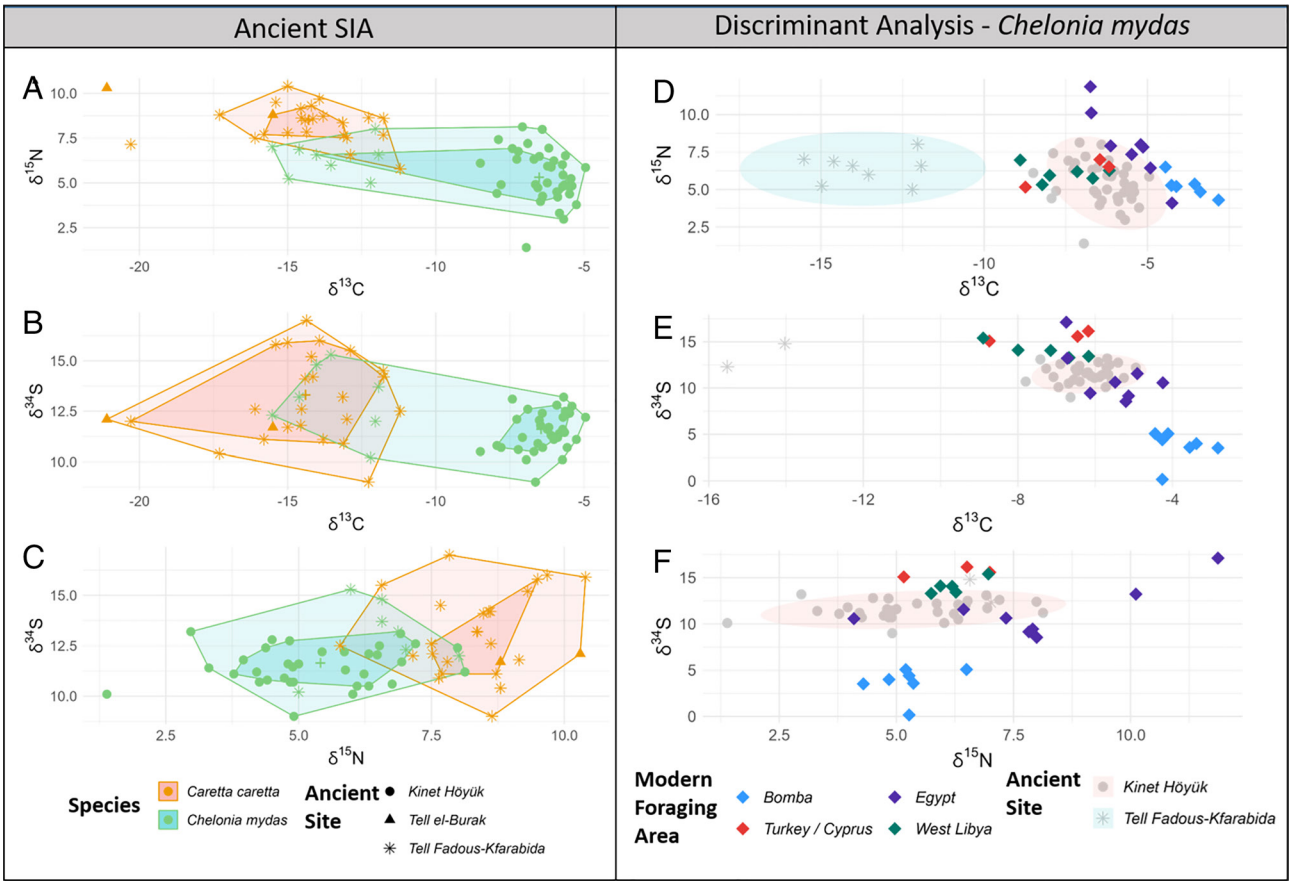

Fig. 4. Mediterranean sea turtle stable isotope values. Ancient SIA bagplots (*A–C*) are of archaeological Levantine sea turtle bones (n = 45). Species identifications are from palaeoproteomics analysis. We also present scatterplots of modern data used in discriminant analysis [*D–F*; ancient *C. mydas* remains (gray points, indicated by ellipses)] overlaid with stable isotope values in samples from [Suess corrected (36)] satellite-tracked modern Levantine *C. mydas* (diamonds). The foraging areas of the modern turtles are Bomba (*n* = 7), Egypt (*n* = 8), Turkey/Cyprus (*n* = 3), and West Libya (*n* = 5). All δ^{34}S data are depicted in plots *A–C*, and δ^{34}S data which passed very stringent (*SI Appendix*) quality filtering in plots *E* and *F* (*n* = 32).

data. The $\delta^{13}C$ values in *C. mydas* from Tell Fadous were considerably lower than the values obtained in the same species from *Kinet Höyük* or the modern Levant (Fig. 4 *A* and *D*), indicating different diets. The native seagrass *Cymodocea nodosa* is the current main diet of Mediterranean *C. mydas* (8), likely due to its high nutritional value (28). The $\delta^{13}C$ values in *C. nodosa* range between –8.2‰ and –6.2‰ in the eastern Mediterranean (29, 30), whereas the range in the endemic seagrass *Posidonia oceanica* is between –15.8‰ and –12‰ (30, 31), similar to many macroalgae and invertebrate species (32). Consequently, it was difficult to infer whether the lower $\delta^{13}C$ values in the ancient Tell Fadous-Kfarabida *C. mydas* remains were of a different seagrass, macroalgae, or omnivory. These remains date to a period characterized by lower temperatures and higher humidity (33, 34). Lower sea surface temperatures have been correlated with an increase in the proportion of animal matter *C. mydas* turtles incorporate into their diets, due to gut microflora potentially functioning less effectively at low temperatures (35). Thus, it is conceivable that climate changes during this period led to a shift in diet from herbivory to some degree of omnivory in the *C. mydas* individuals from Tell Fadous-Kfarabida, which was reflected in the higher $\delta^{15}N$, and depleted $\delta^{13}C$ values observed in this study.

Provenancing Ancient Sea Turtle Foraging Grounds

The provenance of archaeological fish has been inferred using SIA in several studies (37–40), where different bodies of water or seas are compared (e.g., Atlantic vs. Mediterranean). Here, our objective was to identify specific ancient foraging habitats within the same sea basin, never before achieved. We used SIA of $\delta^{13}C$, $\delta^{15}N$ and $\delta^{34}S$ values, and a training dataset from modern satellite tracking (with $\delta^{13}C$ corrected for the Suess effect, *SI Appendix*). Discriminant analysis was used to estimate the posterior probability of foraging ground use by ancient sea turtles. We were able to assign 25 (78%) of 32 archaeological *C. mydas* turtles to a specific foraging ground; 7 to Egypt and 18 to West Libya. The inclusion of $\delta^{34}S$ data in the model greatly improved the overall assignment and confidence rates (Datasets S7 and S8). Although it is unknown whether the Eastern Mediterranean ancient coastal foraging areas were isotopically comparable to their present state, we conclude that ancient *C. mydas* were foraging in areas that were similar to the current Egypt and West Libya foraging grounds.

The spatial differences in $\delta^{34}S$ values among contemporary foraging grounds facilitated the specificity in our habitat assignments of ancient sea turtle samples. The colder and freshwater discharged into both the Adriatic and Aegean Sea is expected to result in isotopic values that are distinct from areas along the North African coast. The contemporary North African lagoons are dominated by *C. nodosa* seagrass meadows (41, 42). *C. nodosa* absorbs sediment sulfide (43) (with lower $\delta^{34}S$ values than seawater) through its roots and eventually becomes incorporated into the leaves (44). The rate of uptake is influenced by temperature, salinity, and the biogeochemical characteristics of the sediment (45). These aspects likely explain why higher $\delta^{34}S$ values have been measured in *C. nodosa* in the Western Mediterranean and Atlantic (46) compared to the Eastern Mediterranean (43). The Western Mediterranean is dominated by water exchange with the North Atlantic Ocean, has had consistent sea surface temperatures and salinity for the previous nine millennia, and consistently lower than that in the eastern basin (currently by ~3 °C and ~2 practical salinity units) (47).

Recent ecological niche modeling showed that the northern Levant and coastal area around Tunisia and West Libya are at high risk of widespread loss of seagrass due to global warming (48, 49). Given the Mediterranean *C. mydas* population's reliance on the seagrass meadows along North Africa during the last ~2,700 y, a period with relatively stable climate, the fate of these crucial marine habitats is of major concern. Our study showed that Mediterranean *C. mydas* have relied upon these areas to sustain breeding for at least ~2,700 y. It follows that the loss of these critical habitats would likely have a major impact on *C. mydas* and thus constitute a serious setback to the current, successful long-term conservation efforts (50). The reduced area of the seagrass meadows that remain will be subjected to higher grazing rates, further exacerbating the overall degradation of these critical marine habitats (51, 52).

We were unable to assign the ancient *C. caretta* samples to specific foraging grounds (*SI Appendix*). It is possible that the more diverse diet and opportunistic feeding of this species (27) will make assignment to highly specific regional foraging grounds from SIA data infeasible (Fig. 4 *A–C* and *SI Appendix*, Fig. S15). However, the large-scale isotopic differences among regions within the Mediterranean Sea suggest that ancient *C. caretta* from the Eastern Mediterranean likely did not forage in the Adriatic Sea. Modern *C. caretta* that are known to feed in the Adriatic Sea had considerably higher $\delta^{15}N$ values than those observed in all other regions in the Mediterranean (22), and higher than the values measured in the ancient *C. caretta* samples analyzed in this study. Contemporary post-nesting *C. caretta* from Cyprus rarely migrate to the Adriatic Sea (22) (in contrast to their counterparts from Western Greece), but feed in the Levantine Sea, as well as along the North African coast, and Tunisian plateau. This, again, draws a parallel between the ancient past and present-day. It is possible that recent anthropogenic alteration of the Adriatic sea (overfishing, nutrient enrichment), which leads to increases in jellyfish blooms (53), has facilitated a recent adoption of this foraging area by *C. caretta* which prey on jellyfish (54). This would indicate that no ancient *C. caretta* populations used the Adriatic; however, the absence of archaeological *C. caretta* remains from other locations prevents us from drawing definitive conclusions. A larger modern dataset of satellite-tracked sea turtles would also aid in the overall assignment of ancient *C. caretta* (and *C. mydas*) samples to specific foraging grounds with higher confidence.

Benefits of Bioarchaeology Data

Our integrative, multidisciplinary, and multitemporal approach facilitated a direct comparison of habitat use by the Mediterranean green sea turtle over thousands of years. This was facilitated by generating data from ancient samples, coupled with modern stable isotope reference datasets from satellite-tracked sea turtles (17, 22). It appears that marine herbivores such as *C. mydas* are particularly suitable to such a comparative study, as its seagrass diet is sessile with high isotopic input from the benthos (44, 55) which results in highly specific consumer isotopic signatures that strongly depend on where foraging occurred. The approach presented is applicable to any migratory marine vertebrate with a high degree of spatial site fidelity to foraging areas with distinctive isotopic profiles and thus provide crucial insights into past habitat use if modern isoscapes are well characterized. This potential is highly valuable due to the relationship between foraging site fidelity and reproductive success in migratory species. The integration of ancient ecological data enabled us to uncover the long-term fidelity of Levantine sea turtles to the Eastern Mediterranean and North African coastal areas in particular. Our study depended on combining ancient and modern data, to identify the species, and subsequently assess long-term foraging ground use. Including historical ecology in conservation studies greatly increases the temporal scale of available data (56), providing baselines for planning and protection measures. The historical abundance, range, and role within an ecosystem are key aspects which can inform

the degree to which a species can return to functionality within its indigenous range (57). Knowing which ecological traits make a species vulnerable allows conservation efforts to be prioritized (58). We argue that in light of our evidence demonstrating millennia-long site fidelity by green turtles to North African seagrass beds, this applied historical ecology study can specifically inform the geographic placement of protected areas.

Conclusions

The results presented here show that Levantine green turtles appear to have utilized the same foraging grounds, and therefore the same migratory routes, along the North African Coast for millennia. The preservation of these seagrass meadows is therefore crucial. Recent environmental modeling studies have shown that seagrass recovery is possible during the next three decades, provided the appropriate protection actions are taken (59). The long-term preservation of these North African seagrass meadows would also conserve an ancient biodiversity heritage. This study shows that bioarchaeology may provide unique insight into "*the effects of multiple stressors on ocean ecosystems*," a priority of the UN Decade of Ocean Science, by providing long-term baselines from which to evaluate the contemporary state of marine biodiversity.

Materials and Methods

Site Information and Specimen Selection.

Museum specimen selection for proteomic references. In order to improve the known *C. caretta* collagen sequence, we took bone samples from 2 *C. mydas* and 4 *C. caretta* specimens from the Groningen Institute for Archaeology Zooarchaeology reference collection, and the Denmark Museum of Zoology. Details can be found in Dataset S3.

Archaeological samples from the levant. Analysed remains from the three archaeological sites most likely derive from exploited breeding or nesting sea turtle populations, as these aggregations would have been easiest to target. Based on regression formulas from breadth of shaft measurements of sea turtle humeri, assumed *C. mydas* from *Kinet Höyük* have curved carapace lengths which range from 64 to 98 cm, and assumed *C. caretta* from Tell Fadous-Kfarabida have a straight carapace length which range from 71 to 78 cm (16), increasing confidence that turtle bones sampled came from adults. Prior to destructive sampling, all bones were scanned using a three dimensional scanner and reconstructed to have a record of the unsampled specimen. Further information about the archaeological sites sea turtle remains come from can be found in ref. 16, and Dataset S1, but we describe them in short:

Kinet Höyük. This site is located in the Gulf of İskenderun, in the northern Levant (Turkey). Sea turtle remains analyzed are from the Middle and Late Iron Ages. In this paper, we refer to the *Kinet Höyük* sea turtles as dating to approximately ~2,700 years B.P.. During this period, sea turtles account for 10.5% of the zooarchaeological assemblage in minimum number of individuals estimates (16). The majority (71%) of bones analyzed here are humeri, some of which had previously been analyzed for species ID via osteology and osteometry (18).

Tell-Fadous-Kfarabida. In the middle Levant (Lebanon), these are the older sea turtle remains we have analyzed, dating to the Early Bronze Age, with few from the Middle Bronze Age. Based on radiocarbon dating (60), we refer to this as approximately ~4,700 years B.P. Analyzed remains from *Tell-Fadous-Kfarabida* are in general more fragmented and composed of elements where osteological species identification is not possible.

Tell el-Burak. Also a Middle Levant archaeological site, we have a considerably smaller assemblage from Tell-el Burak (9 remains analyzed), which all represent remains from the Iron Age II phases A, B, and C. As with *Kinet Höyük*, we refer to this site on average as ~2,700 years B.P.

Protein Extraction and MALDI and LC–MS/MS Spectroscopy.

Sample preparation and protein extraction. Archaeological bone samples were sampled with a dremel, and the surface was cleanly scraped. Analysis was carried out in a keratin-exclusion laboratory at the Globe Institute of the University of Copenhagen. To extract proteins from the bone samples (both ancient and museum reference), we followed a procedure similar to that outlined by Buckley et al. (61). In short, 10 mg of bone was demineralized in 1.2 M HCl and placed on a rotating rack at 4 °C until demineralization was complete. Then, the proteins were extracted using a GuHCL extraction buffer, quantified using a BCA assay, and digested by adding trypsin. Finally, peptides were desalted by ZIPtipping.

MALDI-TOF spectrometry. Samples for ZooMS analysis were spotted out onto a 384-spot MALDI plate and analyzed by MALDI-TOF spectrometry at Cambridge University Bioarchaeology facilities.

LC–MS/MS spectrometry. Additionally, we obtained shotgun proteomic data from the 6 museum reference specimens. These were analyzed by nanoflow liquid chromatography on an EASY-nLC 1,200 coupled to a Q-Exactive HF-X mass spectrometer (Thermo Scientific). For further information on MS parameters, please see study by Mackie et al. (62).

Proteomics Data Analysis.

LC–MS/MS COL1 sequence reconstruction. Spectra were mapped against the complete *C. mydas* COL1 sequence (20) using the pFind software (63). Amino acid substitutions indicated by this step were verified using MaxQuant version 2.0.3.0 (64). We ran both specific and unspecific searches, with the maximum length of peptides in unspecific searches restricted to 40 amino acids. Peptides with good coverage of Y and B ions, especially on the differing amino acid position, were considered reliable. After MaxQuant analysis, we compared the final generated *C. caretta* COL1 sequence with the complete *C. mydas* COL1 sequence. Additional information is provided in *SI Appendix*.

MALDI-TOF ZooMS biomarker analysis. MALDI spectra were observed in the software mMass (65), using established processing criteria (66). In particular, we observed the collagen peaks that should discriminate between *C. mydas* and *C. caretta* according to Harvey et al. (20). We solely used the collagen peptide COL1α1 586-618 (COL1A1T55/56) for species differentiation, due to difficulties with the other two biomarkers (*SI Appendix*). After peptide mass differences were observed in MaxQuant in the reference specimen LC–MS/MS, we observed MALDI spectra for modern and archaeological specimens. If the corresponding m/z peaks were visible in a significant amount of samples, we classified them as a ZooMS biomarker capable of distinguishing between the two species. Additional information is provided in *SI Appendix*.

Analysis of species identifications and method comparisons. We visualized sea turtle species compositions at the three archaeological sites using donut graphs (Fig. 3 *B* and *C*). The success of the unique proteomic species biomarkers was assessed by comparing the number of species identifications achieved, to the numbers achieved using existing sea turtle identification approaches [osteometry and osteology (18), and identification using COL1α1 586 to 618 (20)], barcharts can be viewed in Fig. 3*A*.

Stable Isotope Analysis–Laboratory Methods.

Sample preparation and collagen extraction. Turtle bone samples were cut using a dremel in Groningen, a subset was analyzed in a preliminary isotope study at the Centre for Isotope Research (CIO) in Groningen, and bone material was subsequently sent (December 2020) to the BioArch facilities at the University of York. Collagen extraction at CIO and BioArch facilities both followed respective modified (67) methods. In short, approximately 500 mg of bone was demineralized in acid, gelatinized, and dried. Specifics are described in previous publications (68–70) and are outlined in *SI Appendix*.

Mass Spectrometry. Samples measured at the CIO (5 to 6 mg of collagen) and BioArch (0.5 mg of collagen in duplicate) laboratories were measured by elemental analyzers coupled to continuous-flow isotope ratio mass spectrometers (see *SI Appendix* for equipment models) to achieve $\delta^{13}C$ and $\delta^{15}N$ data. At SUERC, these two instruments were coupled using a continuous flow interface allowing for $\delta^{13}C$, $\delta^{15}N$, and $\delta^{34}S$ signals from the same sample measurement. See *SI Appendix* for further information.

Stable Isotope Analysis–Analysis.

Quality control of ancient SIA data. Samples which failed QC criteria for $\delta^{13}C$ and $\delta^{15}N$ [C:N ratio outside 2.9-3.6 (71)] were excluded from analysis and are not presented. $\delta^{34}S$ quality control was challenging due to the lack of published sulfur quality criteria for ancient reptiles. Here, we use the approach from Rand et al. (25) and allow one diagenic indicator to fall outside the mammalian range for collagen recommended by Nehlich and Richards (26). If more than one QC indicator fell outside the acceptable range, that sample was not used for downstream statistical

analyses; however, it is still displayed (Fig. 3 and Dataset S5). Correlations were also performed between different factors to assess the diagenetic alteration of the bone collagen (*SI Appendix*) as suggested by Bocherens et al. (72). We also visualized SIA data and quality control variables compared to protein concentrations from BCA assays (*SI Appendix*, Fig. S12).

Visualization and analysis of ancient SIA data. RStudio (73), specifically ggplot2 (74), was used for plotting ZooMS and stable isotope data. Bagplots were created for archaeological data using an existing custom *geom_bag* function (*SI Appendix*). Two-sample *t* tests (standard and Welch) were performed to test for statistical differences between the two species, between the two sites *Kinet Höyük* and *Tell-Fadous-Kfarabida*, and between *C. mydas* remains at the two sites. This was preceded by outlier testing (box plots, Rosner's test), Shapiro–Wilk normality tests, and F-tests for homogeneity of variance. In some cases, pseudo-log transformation was required for $\delta^{13}C$ to achieve a normal distribution (*SI Appendix*). Linear regression analysis of $\delta^{13}C$ and $\delta^{15}N$ results was carried out between the three SIA laboratories (*SI Appendix*, Fig. S13), to ensure robustness.

Modern SIA data from satellite-tracked sea turtles. Modern stable isotope training sets from satellite-tracked sea turtles were used to assess posterior probabilities of foraging ground use from the archaeological turtle specimens. The satellite-tracked modern turtle datasets were from homogeneously sampled breeding populations in Cyprus. Methods for acquiring the modern values can be found in refs. 17 and 22 for green and loggerhead turtles, respectively. In short, satellite transmitters were attached to postnesting sea turtles in the Northern Levant, and their migration to a final foraging ground was recorded (*see SI Appendix for further information*). We added custom corrections to the modern $\delta^{13}C$ values, to correct for the depletion in $\delta^{13}C$ which has occurred since the onset of the Industrial Revolution (Suess effect), especially after 1850 (*SI Appendix*).

Discriminant analysis for group assignments. We used RStudio to carry out linear discriminant analysis using the "MASS" package (75) and flexible discriminant analysis using the "mda" package (76) to assign archaeological specimens to modern foraging grounds. The foraging ground distribution of the satellite-tracked training dataset determined the nonuniform priors used in the models. Leave-one-out crossvalidation indicated that the two regions, Turkey-Cyprus and West-Libya, could not be accurately distinguished from each other in the modern green turtle training dataset (Dataset S7). Therefore, we employed a two-step discriminant analysis method for green turtles. First, we carried out Flexible discriminant analysis (FDA) on the ancient test dataset, where the Turkey-Cyprus and West-Libya groups were combined into one group (TCWL) in the training data, as was carried out by Bradshaw et al. (17). We required a minimum posterior probability of 83% to affirm foraging ground membership, as this constitutes an order-of-magnitude (10-fold) increase over random odds (17, 22, 77). Given the nonuniform priors of the green turtle training dataset, this increase varies per foraging area (from 8.7-fold in the most represented foraging site to 10.7-fold in the least represented). Second, the 19 ancient green turtles assigned to TCWL in the first step went through a second FDA which assigned turtles to either Turkey-Cyprus or West-Libya based on $\delta^{34}S$ values. We again required an order-of-magnitude increase from random odds to accept this assignment (posterior probability ≥ 91%). Leave-one-out crossvalidation was used to estimate the accuracy of the predictive models (Dataset S8). R scripts are available on the Zenodo repository (10.5281/zenodo.7886079), along with csv files of input data, to ensure reproducibility of the results.

Data, Materials, and Software Availability. The mass spectrometry proteomics data have been deposited to the ProteomeXchange Consortium via the PRIDE partner repository (78) with the dataset identifier PXD036592. R scripts (79) associated with analysis in this publication have been uploaded to the Zenodo repository (DOI: 10.5281/zenodo.7886079).

ACKNOWLEDGMENTS. We thank M.J. Collins for the opportunity to carry out palaeoproteomics research at The Globe institute. We are grateful to M. Durrant, S. Palstra, M. Munoz-Alegre, R. Winter, A. Andrews, E. Vika, M. Bleasdale, Y. van den Hurk, and S. Vermeersch for laboratory assistance, and A. Giuliani for data analysis support. Many thanks to D. Klingberg Johansson and the National History Museum of Denmark for allowing us to sample sea turtles for proteomic analysis. Discussions with V. Harvey, D. Orton, and O. Türkozan surrounding this work were valuable. Thanks to D. Raemaekers for his supervision of the first author, and S.E. Boersma for map design. Our research would not have been possible without the work of the *Kinet Höyük*, *Tell Fadous-Kfarabida*, and *Tell el-Burak* excavation teams. Special thanks are due to M.-H. Gates, Director of the Kinet Archaeological Project, and S. Ikram. Prof. Jesper Velgaard Olsen at the Novo Nordisk Center for Protein Research is thanked for providing access and resources, which were also funded in part by a donation from the Novo Nordisk Foundation (grant no. NNF14CC0001). Research costs (including the employment of the first author) were funded by the Marie Skłodowska-Curie Innovative Training Network SeaChanges which falls under the European Union's Horizon 2020 research and innovation programme (Marie Skłodowska-Curie grant agreement no. 813383). Several authors were also supported by Danish National Research Foundation grant no. DNRF128 (PROTEIOS). The manuscript was improved as a result of the input of the editor and two reviewers.

Author affiliations: [a]Groningen Institute of Archaeology, Faculty of Arts, University of Groningen, 9712 ER Groningen, Netherlands; [b]Marine Evolution and Conservation Group, Groningen Institute for Evolutionary Life Sciences, Faculty of Science and Engineering, University of Groningen, 9747 AG Groningen, Netherlands; [c]The Globe Institute, Faculty of Health and Medical Science, University of Copenhagen, 1353 Copenhagen K, Denmark; [d]Novo Nordisk Foundation Center for Protein Research, Faculty of Health and Medical Science, University of Copenhagen, 2200 Copenhagen K, Denmark; [e]Trace and Environmental DNA Lab, School of Molecular and Life Sciences, Curtin University, Perth, Western Australia 6102, Australia; [f]Lundbeck Foundation GeoGenetics Centre, GLOBE Institute, University of Copenhagen, 1353 Copenhagen K, Denmark; [g]Centre for Ecology and Conservation, College of Life and Environmental Sciences, University of Exeter, Penryn Campus, Penryn TR10 9FE, United Kingdom; [h]Society for the Protection of Turtles, Nicosia 99150, North Cyprus; [i]Department of History and Archaeology, American University of Beirut, Beirut 1107 2020, Lebanon; [j]BioArCh, Department of Archaeology, University of York, York YO10 5NG, United Kingdom; [k]Centre for Isotope Research, Faculty of Science and Engineering, University of Groningen, 9747 AG Groningen, Netherlands; and [l]Center for Coastal Studies, Provincetown, MA 02657

Author contributions: W.d.K., M.A., A.J.T., and C.Ç. designed research; P.J.P. and C.Ç. acquired funding; W.d.K., M.M., M.R., M.v.T., M.W.D., and A.J.T. performed laboratory research; W.d.K. analyzed data with input from A.C.B., P.J.P., M.A., A.J.T., and C.C., M.E.A. provided access to reference material; A.C.B., J.C.H., B.J.G., R.T.E.S., and P.J.B. provided dataset; H.G. provided access to archaeological samples; W.d.K. and A.J.T. wrote the paper with significant contributions from P.J.P., M.A., and C.Ç.; and M.M., M.R., M.E.A., A.C.B., J.C.H., B.J.G., R.T.E.S., P.J.B., H.G., M.v.T., and M.W.D. read, revised, and agreed to the final manuscript.

1. D. Pauly, Anecdotes and the shifting baseline syndrome of fisheries. *Trends Ecol. Evol.* **10**, 430 (1995).
2. P. K. Dayton, M. J. Tegner, P. B. Edwards, K. L. Riser, Sliding baselines, ghosts, and reduced expectations in kelp forest communities. *Ecol. Appl.* **8**, 309–322 (1998).
3. C. A. Froyd, K. J. Willis, Emerging issues in biodiversity & conservation management: The need for a palaeoecological perspective. *Quat. Sci. Rev.* **27**, 1723–1732 (2008).
4. G. P. Dietl, K. W. Flessa, Conservation paleobiology: Putting the dead to work. *Trends Ecol. Evol.* **26**, 30–37 (2011).
5. A. W. R. Seddon *et al.*, Looking forward through the past: Identification of 50 priority research questions in palaeoecology. *J. Ecol.* **102**, 256–267 (2014).
6. K. L. Stokes *et al.*, Migratory corridors and foraging hotspots: Critical habitats identified for Mediterranean green turtles. *Divers. Distrib.* **21**, 665–674 (2015).
7. L. C. M. Omeyer *et al.*, Investigating differences in population recovery rates of two sympatrically nesting sea turtle species. *Anim. Conserv.* **24**, 832–846 (2021).
8. P. Casale *et al.*, Mediterranean sea turtles: Current knowledge and priorities for conservation and research. *Endanger. Species Res.* **36**, 229–267 (2018).
9. Seminoff; IUCN, (Southwest fisheries science center, U.s.), Chelonia mydas: IUCN Red List of Threatened Species (2004), 10.2305/iucn.uk.2004.rlts.t4615a11037468.en.
10. Casale, Tucker; IUCN, *Caretta caretta* (amended version of 2015 assessment) IUCN Red List of Threatened Species (2015), 10.2305/iucn.uk.2017-2.rlts.t3897a119333622.en.
11. C. J. A. Bradshaw, M. A. Hindell, M. D. Sumner, K. J. Michael, Loyalty pays: Potential life history consequences of fidelity to marine foraging regions by southern elephant seals. *Anim. Behav.* **68**, 1349–1360 (2004).
12. Y. Aharon-Rotman, K. L. Buchanan, N. J. Clark, M. Klaassen, W. A. Buttemer, Why fly the extra mile? Using stress biomarkers to assess wintering habitat quality in migratory shorebirds *Oecologia* **182**, 385–395 (2016).
13. S. C. Patrick, H. Weimerskirch, Reproductive success is driven by local site fidelity despite stronger specialisation by individuals for large-scale habitat preference. *J. Anim. Ecol.* **86**, 674–682 (2017).
14. T. Shimada *et al.*, Fidelity to foraging sites after long migrations. *J. Anim. Ecol.* **89**, 1008–1016 (2020).
15. A. C. Broderick, M. S. Coyne, W. J. Fuller, F. Glen, B. J. Godley, Fidelity and over-wintering of sea turtles. *Proc. Biol. Sci.* **274**, 1533–1538 (2007).
16. C. Çakırlar, F. J. Koolstra, S. Ikram, Tracking turtles in the past: Zooarchaeological evidence for human-turtle interactions in the ancient Eastern Mediterranean. *Antiquity* **95**, 125–141 (2021).
17. P. J. Bradshaw *et al.*, Satellite tracking and stable isotope analysis highlight differential recruitment among foraging areas in green turtles. *Mar. Ecol. Prog. Ser.* **582**, 201–214 (2017).

18. F. J. Koolstra, H. C. Küchelmann, C. Cakirlar, Comparative osteology and osteometry of the coracoideum, humerus, and femur of the green turtle (Chelonia mydas) and the loggerhead turtle (Caretta caretta). *Int. J. Osteoarchaeol.* **29**, 683–695 (2019), 10.1002/oa.2761.
19. R. M. Winter, W. de Kock, P. J. Palsbøll, C. Çakirlar, Potential applications of biomolecular archaeology to the ecohistory of sea turtles and groupers in Levant coastal antiquity. *J. Archaeol. Sci. Rep.* **36**, 102872 (2021).
20. V. L. Harvey *et al.*, Preserved collagen reveals species identity in archaeological marine turtle bones from Caribbean and Florida sites. *R. Soc. Open Sci.* **6**, 191137 (2019).
21. M. Buckley, "Zooarchaeology by mass spectrometry (ZooMS) collagen fingerprinting for the species identification of archaeological bone fragments" in *Zooarchaeology in Practice: Case Studies in Methodology and Interpretation in Archaeofaunal Analysis* (Springer, Cham, 2017), pp. 227–247.
22. J. C. Haywood *et al.*, Spatial ecology of loggerhead turtles: Insights from stable isotope markers and satellite telemetry. *Divers. Distrib.* **26**, 368–381 (2020).
23. C. N. Turner Tomaszewicz, J. A. Seminoff, S. H. Peckham, L. Avens, C. M. Kurle, Intrapopulation variability in the timing of ontogenetic habitat shifts in sea turtles revealed using δ15 N values from bone growth rings. *J. Anim. Ecol.* **86**, 694–704 (2017).
24. C. N. Turner Tomaszewicz, J. A. Seminoff, L. Avens, C. M. Kurle, Methods for sampling sequential annual bone growth layers for stable isotope analysis. *Methods Ecol. Evol.* **7**, 556–564 (2016).
25. A. J. Rand, C. Freiwald, V. Grimes, A multi-isotopic (δ13C, δ15N, and δ34S) faunal baseline for Maya subsistence and migration studies. *J. Archaeol. Sci. Rep.* **37**, 102977 (2021).
26. O. Nehlich, M. P. Richards, Establishing collagen quality criteria for sulphur isotope analysis of archaeological bone collagen. *Archaeol. Anthropol. Sci.* **1**, 59–75 (2009).
27. J. L. Palmer *et al.*, Dietary analysis of two sympatric marine turtle species in the eastern Mediterranean. *Mar. Biol.* **168**, 94 (2021).
28. C. Marco-Méndez *et al.*, Epiphyte presence and seagrass species identity influence rates of herbivory in Mediterranean seagrass meadows. *Estuar. Coast. Shelf Sci.* **154**, 94–101 (2015).
29. W. de Kock, H. Hasler-Sheetal, M. Holmer, M. Tsapakis, E. T. Apostolaki, Metabolomics and traditional indicators unveil stress of a seagrass (Cymodocea nodosa) meadow at intermediate distance from a fish farm. *Ecol. Indic.* **109**, 105765 (2020).
30. E. T. Apostolaki *et al.*, Exotic Halophila stipulacea is an introduced carbon sink for the Eastern Mediterranean Sea. *Sci. Rep.* **9**, 9643 (2019).
31. E. T. Apostolaki *et al.*, The importance of dead seagrass (Posidonia oceanica) matte as a biogeochemical sink. *Front. Marine Sci.* **9**, 861998 (2022).
32. J. K. Pinnegar, N. V. C. Polunin, Contributions of stable-isotope data to elucidating food webs of Mediterranean rocky littoral fishes. *Oecologia* **122**, 399–409 (2000).
33. P. M. Fischer, *Tell Abu Al-Kharaz in the Jordan Valley* (Austrian Academy of Sciences Press, 2006).
34. D. Langgut, I. Finkelstein, T. Litt, F. H. Neumann, M. Stein, Vegetation and climate changes during the Bronze and Iron ages (~3600–600 BCE) in the Southern levant based on palynological records. *Radiocarbon* **57**, 217–235 (2015).
35. N. Esteban *et al.*, A global review of green turtle diet: Sea surface temperature as a potential driver of omnivory levels. *Mar. Biol.* **167**, 183 (2020).
36. G. Sisma-Ventura, R. Yam, A. Shemesh, Recent unprecedented warming and oligotrophy of the eastern Mediterranean Sea within the last millennium. *Geophys. Res. Lett.* **41**, 5158–5166 (2014).
37. L. Llorente-Rodríguez *et al.*, Elucidating historical fisheries' networks in the Iberian Peninsula using stable isotopes. *Fish Fish* **23**, 862–873 (2022), 10.1111/faf.12655.
38. J. H. Barrett *et al.*, Interpreting the expansion of sea fishing in medieval Europe using stable isotope analysis of archaeological cod bones. *J. Archaeol. Sci.* **38**, 1516–1524 (2011).
39. E. J. Guiry *et al.*, Evidence for freshwater residency among Lake Ontario Atlantic salmon (Salmo salar) spawning in New York. *J. Great Lakes Res.* **46**, 1036–1043 (2020).
40. S.-V. Guy *et al.*, Tooth oxygen isotopes reveal Late Bronze Age origin of Mediterranean fish aquaculture and trade. *Sci. Rep.* **8**, 14086 (2018).
41. Y. A. Geneid, H. H. El-Hady, Distribution, biomass and biochemical contents of the seagrass species of Lake Bardawil, Mediterranean Sea. *Egypt. Biol. Mar. Medit.* **13**, 226–229 (2006).
42. G. Pergent *et al.*, Characterization of the benthic vegetation in the Farwà Lagoon (Libya). *J. Coast. Conserv.* **8**, 119–126 (2002).
43. E. T. Apostolaki, M. Holmer, V. Santinelli, I. Karakassis, Species-specific response to sulfide intrusion in native and exotic Mediterranean seagrasses under stress. *Mar. Environ. Res.* **134**, 85–95 (2018).
44. M. Holmer, H. Hasler-Sheetal, Sulfide intrusion in seagrasses assessed by stable sulfur isotopes–a synthesis of current results. *Front. Marine Sci.* **1**, 64 (2014).
45. M. S. Koch, S. A. Schopmeyer, M. Holmer, C. J. Madden, C. Kyhn-Hansen, Thalassia testudinum response to the interactive stressors hypersalinity, sulfide and hypoxia. *Aquat. Bot.* **87**, 104–110 (2007).
46. O. Mascaró, S. Oliva, M. Pérez, J. Romero, Spatial variability in ecological attributes of the seagrass *Cymodocea nodosa*. *Botanica Marina* **52**, 429–438 (2009).
47. K.-C. Emeis *et al.*, Temperature and salinity variations of Mediterranean Sea surface waters over the last 16,000 years from records of planktonic stable oxygen isotopes and alkenone unsaturation ratios. *Palaeogeogr. Palaeoclimatol. Palaeoecol.* **158**, 259–280 (2000).
48. R. M. Chefaoui, C. M. Duarte, E. A. Serrão, Dramatic loss of seagrass habitat under projected climate change in the Mediterranean Sea. *Glob. Chang. Biol.* **24**, 4919–4928 (2018).
49. S. Pruckner, J. Bedford, L. Murphy, J. A. Turner, J. Mills, Adapting to heatwave-induced seagrass loss: Prioritizing management areas through environmental sensitivity mapping. *Estuar. Coast. Shelf Sci.* **272**, 107857 (2022).
50. J. A. Camiñas *et al.*, "Conservation of marine turtles in the Mediterranean sea" (International Union for Conservation of Nature, 2020), 10.13140/RG.2.2.33111.19368.
51. M. R. Heithaus *et al.*, Seagrasses in the age of sea turtle conservation and shark overfishing. *Front. Marine Sci.* **1**, 28 (2014).
52. M. J. A. Christianen *et al.*, Habitat collapse due to overgrazing threatens turtle conservation in marine protected areas. *Proc. Biol. Sci.* **281**, 20132890 (2014).
53. T. Falkenhaug, Review of jellyfish blooms in the Mediterranean and black sea. *Mar. Biol. Res.* **10**, 1038–1039 (2014).
54. B. Sala, A. Balasch, E. Eljarrat, L. Cardona, First study on the presence of plastic additives in loggerhead sea turtles (Caretta caretta) from the Mediterranean Sea. *Environ. Pollut.* **283**, 117108 (2021).
55. N. Marbà *et al.*, Carbon and nitrogen translocation between seagrass ramets. *Mar. Ecol. Prog. Ser.* **226**, 287–300 (2002).
56. C. Peters, K. K. Richter, J.-C. Svenning, N. Boivin, Leveraging palaeoproteomics to address conservation and restoration agendas. *iScience* **25**, 104195 (2022).
57. M. Grace *et al.*, Using historical and palaeoecological data to inform ambitious species recovery targets. *Philos. Trans. R. Soc. Lond. B Biol. Sci.* **374**, 20190297 (2019).
58. D. A. Fordham *et al.*, Predicting and mitigating future biodiversity loss using long-term ecological proxies. *Nat. Clim. Chang.* **6**, 909–916 (2016).
59. C. M. Duarte *et al.*, Rebuilding marine life. *Nature* **580**, 39–51 (2020).
60. F. Höflmayer, M. W. Dee, H. Genz, S. Riehl, Radiocarbon evidence for the early Bronze Age levant: The site of tell Fadous-Kfarabida (Lebanon) and the end of the early Bronze III period. *Radiocarbon* **56**, 529–542 (2014).
61. M. Buckley, M. Collins, J. Thomas-Oates, J. C. Wilson, Species identification by analysis of bone collagen using matrix-assisted laser desorption/ionisation time-of-flight mass spectrometry. *Rapid Commun. Mass Spectrom.* **23**, 3843–3854 (2009).
62. M. Mackie *et al.*, Palaeoproteomic profiling of conservation layers on a 14th century Italian wall painting. *Angew. Chem. Int. Ed. Engl.* **57**, 7369–7374 (2018).
63. L.-H. Wang *et al.*, pFind 2.0: A software package for peptide and protein identification via tandem mass spectrometry. *Rapid Commun. Mass Spectrom.* **21**, 2985–2991 (2007).
64. J. Cox, M. Mann, MaxQuant enables high peptide identification rates, individualized p.p.b.-range mass accuracies and proteome-wide protein quantification. *Nat. Biotechnol.* **26**, 1367–1372 (2008).
65. M. Strohalm, D. Kavan, P. Novák, M. Volný, V. Havlícek, mMass 3: A cross-platform software environment for precise analysis of mass spectrometric data. *Anal. Chem.* **82**, 4648–4651 (2010).
66. A. Janzen *et al.*, Distinguishing African bovids using Zooarchaeology by Mass Spectrometry (ZooMS): New peptide markers and insights into Iron Age economies in Zambia. *PLoS One* **16**, e0251061 (2021).
67. R. Longin, New method of collagen extraction for radiocarbon dating. *Nature* **230**, 241–242 (1971).
68. M. W. Dee *et al.*, Radiocarbon dating at Groningen: New and updated chemical pretreatment procedures. *Radiocarbon* **62**, 63–74 (2020).
69. M. M. Alexander, C. M. Gerrard, A. Gutiérrez, A. R. Millard, Diet, society, and economy in late medieval Spain: Stable isotope evidence from Muslims and Christians from Gandía, Valencia. **156**, 263–273 (2015).
70. K. L. Sayle, C. R. Brodie, G. T. Cook, W. D. Hamilton, Sequential measurement of δ15 N, δ13 C and δ34 S values in archaeological bone collagen at the Scottish Universities Environmental Research Centre (SUERC): A new analytical frontier. *Rapid Commun. Mass Spectrom.* **33**, 1258–1266 (2019).
71. M. J. DeNiro, Postmortem preservation and alteration of in vivo bone collagen isotope ratios in relation to palaeodietary reconstruction. *Nature* **317**, 806–809 (1985).
72. H. Bocherens, D. G. Drucker, H. Taubald, Preservation of bone collagen sulphur isotopic compositions in an early Holocene river-bank archaeological site. *Palaeogeogr. Palaeoclimatol. Palaeoecol.* **310**, 32–38 (2011).
73. RStudio Team, RStudio: Integrated Development Environment for R (Version 4.1.1, Posit Software, PBC, Boston, MA, 2020).
74. H. Wickham, *ggplot2 Elegant Graphics for Data Analysis* (Springer International Publishing, ed. 2, 2016) (22 June 2022).
75. W. N. Venables, B. D. Ripley, *Modern Applied Statistics with S* (Springer, New York, NY, 2002).
76. T. Hastie, R. Tibshirani, J. H. Friedman, (Springer, ed. 2, 2009). 10.1007/b94608.
77. H. B. Vander Zanden *et al.*, Determining origin in a migratory marine vertebrate: A novel method to integrate stable isotopes and satellite tracking. *Ecol. Appl.* **25**, 320–335 (2015).
78. Y. Perez-Riverol *et al.*, The PRIDE database and related tools and resources in 2019: Improving support for quantification data. *Nucleic Acids Res.* **47**, D442–D450 (2019).
79. W. de Kock, Analysis - Threatened North African seagrass meadows have supported green turtle populations for millennia. *Zenodo*. https://doi.org/10.5281/zenodo.7886079. Deposited 2 May 2023.